Proton beam dosimetry at ultra-high dose rates (FLASH): Evaluation of GAFchromic™ (EBT3, EBT-XD) and OrthoChromic (OC-1) film performances

Daphnée Villoing, Charbel Koumeir, Arthur Bongrand, Arnaud Guertin, Ferid Haddad, Vincent Métivier, Freddy Poirier, Vincent Potiron, Noël Servagent, Stéphane Supiot, et al.

Proton beam dosimetry at ultra-high dose rates (FLASH): evaluation of GAFchromic™ (EBT3, EBT-XD) and OrthoChromic (OC-1) film performances.

Short running title: Radiochromic film in UHDR proton therapy

Author list: Daphnée Villoing[1], Charbel Koumeir[2], Arthur Bongrand[2], Arnaud Guertin[3], Ferid Haddad[2,3], Vincent Métivier[3], Freddy Poirier[2], Vincent Potiron[1], Noël Servagent[3], Stéphane Supiot[1], Grégory Delpon[1,3], Sophie Chiavassa[1,3]

[1] Institut de Cancérologie de l'Ouest, Saint-Herblain, France

[2] GIP ARRONAX, Saint-Herblain, France

[3] Laboratoire SUBATECH, UMR 6457, CNRS IN2P3, IMT Atlantique, Université de Nantes, France

For correspondence:

Sophie Chiavassa, PhD

Institut de Cancérologie de l'Ouest, Bd Professeur Jacques Monod, 44800 Saint-Herblain, France

E-mail : sophie.chiavassa@ico.unicancer.fr, Phone number : (+33)240679963

Manuscript type: Technical Note

Abstract (max 300 words)

Purpose:

The ARRONAX cyclotron facility offers the possibility to deliver proton beams from low to ultra-high dose rates (UHDR). As a good control of the dosimetry is a prerequisite of UHDR experimentations, we evaluated in different conditions the usability and the dose rate dependency of several radiochromic films commonly used for dosimetry in radiotherapy.

Methods:

We compared the dose rate dependency of three types of radiochromic films: EBT3 and EBT-XD (GAFchromic™), and OC-1 (OrthoChrome Inc.), after proton irradiations at various mean dose rates (0.25, 40, 1500 and 7500 Gy/s) and for 10 doses (2–130 Gy). We also evaluated the dose rate dependency of each film considering beam structures, from single pulse to multiple pulses with various frequencies.

Results:

EBT3 and EBT-XD films showed differences of response between conventional (0.25 Gy/s) and UHDR (7500 Gy/s) conditions, above 10 Gy. On the contrary, OC-1 films did not present overall difference of response for doses except below 3 Gy. We observed an increase of the netOD with the mean dose rate for EBT3 and EBT-XD films. OC-1 films did not show any impact of the mean dose rate up to 7500 Gy/s, above 3 Gy. No difference was found based on the beam structure, for all three types of films.

Conclusions:

EBT3 and EBT-XD radiochromic films should be used with caution for the dosimetry of UHDR proton beams over 10 Gy. Their overresponse, which increases with mean dose rate and dose, could lead to non-negligible overestimations of the absolute dose. OC-1 films are dose rate independent up to 7500Gy/s in proton beams. Films response is not impacted by the beam structure. A broader

investigation of the usability of OC-1 films in UHDR conditions should be conducted at intermediate and higher mean dose rates and other beam energies.

Keywords: Radiochromic films, proton beam therapy, film dosimetry, FLASH, ultra-high dose rates

1. Introduction

The radiobiological effectiveness of an irradiation strongly depends on the radiation dose, the fractionation and the dose rate. Already in the 1960s, Berry et al. [1] demonstrated an improvement of cell survival when delivering the total amount of radiation dose within only a single nanosecond-length pulse of photons, compared to conventional RT. In recent years, the use of ultra-high dose rates (UHDR), typically above 40 Gy/s, has showed promising results, reducing side effects to healthy tissues while effectively allowing the tumor control [2–6]. This effect, named FLASH, has first been observed *in vitro* with X rays [1], electrons [7], and more recently with proton beams [8]. *In vivo* preclinical studies also demonstrated a FLASH effect: significant normal tissue sparing was noticed using electron beams in mouse [9–11], zebrafish embryos [5,12], mini-pig and cat [4], while tumor control remained as efficient. Recently, a FLASH effect was observed in mice using a 230 MeV proton beam in UHDR conditions [13].

In an effort to fully comprehend the differential effect of FLASH irradiation in tumor and normal tissue, one major prerequisite is to control the dosimetry, in both conventional and UHDR conditions. Ionization chambers are commonly used for reference dosimetry in external beam RT, following IAEA TRS-398 reference recommendations [14]. However, the reliability of ionization chambers starts to fail for higher dose rate (or dose rate-per-pulse) beams, as the ion recombination between the electrodes exceeds a saturation level [15–17]. Therefore, it is essential to ascertain an accurate method of determination of the dose in UHDR conditions.

Among the range of detectors available for reference dosimetry, radiochromic films such as EBT3 Gafchromic™ films have commonly been used for dose verification in external beam RT, including Proton RT [18,19]. Therefore, their suitability for reference dose measurements in UHDR conditions has been studied in various beam setups. Karsch *et al.* [20] investigated the dose rate dependency of previous generations of Gafchromic™ films (EBT) using a 20 MeV pulsed electron beam and found no dependency with dose-rates in pulse up to 15 x 10^9 Gy/s within 5%. More recently, Jaccard *et al.* [21] established that EBT3 Gafchromic™ films were dose-rate independent for pulsed electron beams with dose-rates in pulse up to 8 x10^6 Gy/s, within 4% uncertainty. Jorge *et al.* [22] showed similar results with

both EBT3 and EBT-XD Gafchromic™ films, when delivering 6 MeV pulsed electron beams at dose rates up to 1050 Gy/s. Favaudon *et al.* [23] observed the same response with EBT3 films over a wide range of dose rates, for doses from 1 mGy to over 30 Gy per microsecond pulse. As to their suitability for proton beam dosimetry, Patriarca *et al.* [24] observed consistent results between EBT3 films and a CC01 chamber for dose rates of 40 Gy/s, in the plateau of a 198 MeV Bragg peak. EBT3 Gafchromic™ films were also used for the control dosimetry of 200–250 MeV proton beams at dose rates of 100–120 Gy/s [25–27], and unlaminated EBT3 films for a 4.5 MeV proton beam, at dose rates up to 1000 Gy/s [28]. However, to date, the dose rate independency of radiochromic films has only been established for low-energy proton beams, or for high-energy proton beams at the lower dose-rate bound of UHDR conditions (~ 40 Gy/s).

In the present study, we evaluated the dose rate dependency of three different types of radiochromic films for the dosimetry of 68 MeV proton beams in UHDR conditions, considering various mean dose rates and beam structures.

2. Material and Methods

For the reader's convenience, we followed the terminology from Esplen *et al.* [29] throughout this study to describe the beam structure.

2.A. The proton beamline

2.A.1. ARRONAX facility

ARRONAX is an isochronous cyclotron (IBA Cyclone 70XP) that partially serves as a user facility for research[30]. This cyclotron produces protons from 30 MeV up to 70 MeV, deuterons from 15 MeV up to 35 MeV and alpha particles at a fixed energy of 68 MeV. Proton beams can be designed from low (<1 pA) to high (up to 350 µA) intensities, using bunches of protons interspaced by 32.84 ns (micro-pulse, RF = 30.45 MHz). The ARRONAX cyclotron offers the possibility of delivering a given dose in a wide range of dose rates from low to ultra-high dose rates. A homemade pulsing chopper-based system was developed and validated [31,32], in order to adjust the duration of the irradiation (>10 µs) and

the frequency rate of the macro-pulse repetition, allowing an easy shift between conventional and UHDR irradiations and a flexible beam structure.

2.A.2. Experimental setup

Our experimental setup, with a nominal beam energy of 68 MeV, is adapted to preclinical irradiations of cells or small animals [33]. A 52-µm tungsten foil and two aluminum collimators (Ø 15 and 10 mm) are used to spread and homogenize the beam. Two types of detectors were installed on the beamline for relative real-time dosimetry: a photomultiplier (PM) tube (model R928, Hamamatsu Photonics, France) measuring the UV photons emitted from excited nitrogen created by the interaction of the air with the incident beam along its path [34], and an in-transmission parallel-plate ionization chamber (IC) (model 34058, PTW, Freiburg, Germany). Specific calibrations of the PM tube and the IC are performed at the beginning of each experiment using a Faraday cup (FC) with its suppressor ring, placed after the target, and a high-precision electrometer (model Multidos, PTW, Freiburg, Germany). The delivered dose at the irradiation point was determined as defined by Koumeir *et al* [30]:

$$D[Gy] = F[cm^{-2}] \cdot \mathrm{S(E)}[\mathrm{MeV} \cdot cm^2 \cdot g^{-1}] \times 1.6 \times 10^{-10}$$

Where F is the fluence – obtained from the electric charge reading – of the protons in our 10-mm diameter beam spot and $\mathrm{S(E)}$ the stopping power.

In this study, doses from UHDR irradiations were calculated using electric charge readings from the PM (rise time ~2 ns), while those from conventional irradiations were calculated using readings from the IC. With this setup, the proton beam spot has a 10-mm diameter at the target position. Our experimental setup is detailed in **Figure 1**.

To repeat the irradiation at different doses and dose rates with identical positioning of the target, an in-house automatic XY linear translator was built using a high-precision two-axis stage with step motor. More detailed information is available in 2.C.

2.B. Radiochromic films

2.B.1. Film composition and properties

Three types of radiochromic films were compared in this study: GAFchromic™ EBT3 (lot: 11192001) and GAFchromic™ EBT-XD (lot: 11062002), manufactured by Ashland Inc. (Wayne, NJ, USA) and OrthoChromic OC-1 (lot: 2-20200131-1), manufactured by Orthochrome Inc. (Hillsborough, NJ, USA).

Both EBT3 and EBT-XD films comprise a single active layer, 28-µm and 25-µm thick, respectively, sandwiched between two 125-µm matte surface clear polyester bases [35,36]. The active layer contains an active component, a marker dye, stabilizers and other components providing the film with a low-energy dependency. The yellow marker dye, in conjunction with an RGB film scanner, enables the dosimetry process to benefit from the application of multichannel dosimetry. In addition to the active layer thickness, EBT-XD films slightly differ from EBT3 in their chemical composition (**Appendix 1**). Unlike EBT3 and EBT-XD, OC-1 films lack the polyester laminate on one side, thus exposing directly the 30-µm thick active layer [37]. It is opaque, whereas the two GAFchromic™ films are transparent.

Dynamic dose ranges of EBT3, EBT-XD and OC-1 films spread from 0.1 Gy to 20, 60 and 100 Gy, respectively. Properties of these films are summarized in **Appendix 2**.

After irradiation, each film was horizontally cut in landscape orientation in four sub-sections for later scanning and stored at room temperature in lightproof envelopes.

2.B.2. Film reading

All films were digitized between 24 and 48h after their irradiation, using a V700 Photo Epson Perfection flatbed color scanner (Epson America Inc., CA, USA). Five scans were consistently performed prior to any film scan in order to warm up the scan lamp. Each sub-section of the film was systematically scanned in landscape orientation, with all image enhancement filters turned off, positive 48 bits-colors (16-bit per color channel) and a resolution of 72 dots per inch. The transmission mode was used for EBT3 and EBT-XD films, whereas OC-1 films were scanned in reflection mode. Each image was stored in a Tagged Image File Format (TIFF) file.

2.B.3. Film analysis

The response of the film was assessed using the net optical density defined as follows:

$$netOD = log\left(\frac{I_0}{I}\right)$$

Where I_0 is the mean pixel value (MPV) of unexposed regions of interest (ROIs) of the film and I is the MPV of irradiated ROIs of the film.

Using ImageJ software v1.53e (National Institutes of Health, USA), MPVs and associated standard deviations were then measured on both red and green channels on 4.94-mm diameter ROIs, centered on each irradiated spot for the determination of I. MPVs of five different unexposed parts of each of the four sub-sections of the film were averaged to obtain an overall I_0 for each film.

2.C. Experiments

In all our experiments, an Eppendorf tubes rack – previously designed and 3D-printed for separate experiments on Zebrafish embryos – was used as a film holder. A stack of films was positioned at the entrance of this rack in the following order along the beam axis: EBT3, EBT-XD and OC-1. The positioning of each irradiation was remotely controlled using our in-house automatic XY translator, previously calibrated for 20 possible specific positions in X and Y, designated by line number (1–4) and column letter (A–E). The dose range selected for our experiments was set to exceed the widest dynamic dose range of the three types of films, therefore that of OC-1 films (0.1 – 100 Gy).

2.C.1. Conventional vs. UHDR

In experiment #1, we evaluated the difference of film response between conventional (~ 0.25 Gy/s) and UHDR (~ 7500 Gy/s) for ten different doses from ~ 2 to 130 Gy. All UHDR irradiations were conducted using a single macro-pulse with a variable width (0.27–16.67 ms), whereas conventional irradiations were performed delivering 800 to 50,000 successive macro-pulses with a 0.4-ms width and a frequency of 100 Hz. The beam structures in use are described in **Table 1** and **Figure 2**.

2.C.2. Variation of the mean dose rate

In experiment #2, three series of ten irradiations (from ~ 2 to 130 Gy) were performed with mean dose rates, considered ultra-high, of 40 Gy/s, 1500 Gy/s and 7500 Gy/s, using a single macro-pulse with variable widths of 75–3000 ms, 2–80 ms and 0.27–16.67 ms, respectively (**Table 1** and **Figure 2B**).

2.C.3. Variation of the beam structure

In experiment #3, two series of ten multi-pulse irradiations (from ~ 2 to 130 Gy) were conducted with intra-pulse dose rates of 7500 Gy/s (pulse width = 100 μs), using number of macro-pulses varying between 4 and 160 and a frequency of 53.3 and 2000 Hz to obtain mean dose rates of 40 and 1500 Gy/s, respectively (**Table 1** and **Figure 2C**).

2.D. Uncertainty analysis

Two main sources of uncertainty must be evaluated in this study: the uncertainty on the dose, as determined at the calibration time, and the uncertainty on the measured netOD. An uncertainty on the dose of 1.5% was assessed in conventional mode with the IC, whereas it was estimated to be 3.0% in UHDR with the PM. The uncertainty on the measured netOD was expressed as the combination of four different components, following Jaccard *et al.* [21]. The intra-film uniformity $u_I^{uniformity}$ was evaluated comparing the mean pixel values in five different localizations of the same film after irradiation with the same dose. The local film uniformity u_I^{local} was assessed by calculating the standard deviation on pixel values in the regions of interest used for dosimetry. The scanner repeatability u_I^{scan} was evaluated by comparing the mean pixel values after scanning three times in a row the exact same region of interest on the film. Finally, the uncertainty on the scanner positioning $u_I^{position}$ was calculated by comparing the mean pixel values of a similar region of interest after independently repeating three times the scanning process. Combining all sources of uncertainty, we estimated an overall uncertainty u_I^{total} (%) on the netOD for each type of film and for red and green channel.

$$u_I^{total} = \sqrt{u_I^{uniformity^2} + u_I^{local^2} + u_I^{scan^2} + u_I^{position^2}}$$

Combining all sources of uncertainty, we found overall uncertainties u_I^{total} (%) on the netOD of [1.63 – 3.34], [1.44 – 5.12] and [1.85 – 13.31] %, respectively for EBT3, EBT-XD and OC-1 films. Detailed values of uncertainty by film, channel, dose range (≤10 Gy, or > 10 Gy) and source of uncertainty are listed in **Appendix 3**.

2.E. Statistical analysis

During our irradiations, we aimed at reaching ten specific dose values. However, the conditions of irradiations, which depend on the beam stability, do not always allow to precisely reach the targeted dose value.

In order to evaluate the significance of possible differences between our series of netOD as a function of the dose, as dose values vary from one distribution to another, part of our data was fitted with the following function [21]:

$$netOD = ln\left(\frac{a + b \cdot D}{c + D}\right)$$

Where a, b and c are constants, and D is the dose.

The method of maximum likelihood estimation (MLE) was used to fit our data with the Excel solver, and each series of irradiation was divided into three dose sections (2–20; 20–50; 50–130 Gy) to optimize the quality of each fit.

Relative differences in the netOD between various series of irradiations were compared to the corresponding uncertainty levels, for each type of film and channel. Relative differences were considered significant when superior to twice the respective uncertainty.

3. Results

3.A Conventional vs. UHDR

With our experiment #1, we evaluated in the entrance of the Bragg plateau the differences in film response between conventional (0.25 Gy/s) and UHDR (7500 Gy/s), for EBT3, EBT-XD and OC-1 films, using the red (**Figure 3**) and green (**Appendix 4**) channels of these films.

EBT3 films did not show significant relative differences in the netOD between conventional and UHDR irradiations up to 30 Gy for the red channel and up to 10 Gy for the green channel. Relative differences of 3.6–6.0% were observed above 40 Gy for the red channel and 6.6–9.1% were found above 20 Gy for the green channel.

For EBT-XD films, relative differences in the netOD were found significant above 20 Gy with 2.9–4.6%, using the red channel, except for one dose point (40.4 Gy). Using the green channel, relative differences were consistently found significant (4.9–11.4%) except at 4.9 Gy.

OC-1 films showed different results: relative differences in the netOD between conventional and UHDR irradiations were not found significant using either red or green channels, except for the lowest dose point (2.3 Gy), with 14% and 39% of relative difference for red and green channels, respectively.

3.B Variation of the mean dose rate

With experiment #2, using a single macro-pulse, the mean dose rate is equal to the intra-pulse dose rate. The dependency of the films to the mean dose rate was evaluated using non-conventional dose rates of 40 Gy/s, 1500 Gy/s and 7500 Gy/s (**Figure 4**).

For EBT3 and EBT-XD films, the netOD was observed to be increasing with the mean dose rate. For EBT3, between 40 Gy/s and 7500 Gy/s, relative differences in netOD were consistently found significant with 4.1–14.2% and 8.1–12.2% for red and green channels, respectively, except for the lowest dose point (3.2 Gy), using the red channel. Relative differences between 1500 and 40 Gy/s were found significant for 10, 19, 101 and 129 Gy, reading the red channel, and for 19, 29 and 81 Gy, reading the green channel.

For EBT-XD, relative differences in the netOD between 40 Gy/s and 7500 Gy/s were not found significant for 16.4 Gy and below, using both channels. For higher doses, the netOD was observed to be increasing with the mean dose rate, with relative differences of 3.0–5.6% and 3.6–7.7%, using red and green channels, respectively. Relative differences in the netOD were more rarely found significant between 40 and 1500 Gy/s.

For OC-1 films, the netOD was overall not observed to be significantly increasing with the mean dose rate. The only significant relative differences in netOD were observed between 40 and 7500 Gy/s for the lowest dose point (3.2 Gy) using both the red and green channels, and at 16.4 Gy (green channel).

3.C Variation of the beam structure

With experiment #3, the impact of the structure was evaluated on the films by comparing the netOD values between a mean dose rate of 40 Gy/s produced with a single macro-pulse (intra-pulse dose rate of 40 Gy/s) and with multiple macro-pulses (repetition of ten macro-pulses with an intra-pulse dose rate of 7500 Gy/s) (**Figure 5**), and between 1500 Gy/s with a single macro-pulse and with multiple macro-pulses (**Appendix 5**).

For EBT3 films, at a mean dose rate of 40 Gy/s, relative differences in the netOD were never found significant between a single macro-pulse and multiple macro-pulses, using either the red or green channels. Similar results were observed at 1500 Gy/s, except for the lowest dose point (2.9 Gy) where relative differences in the netOD were found significant, with 5.4 and 7.3% using the red and green channels, respectively.

Similarly, EBT-XD and OC-1 films did not show significant relative differences between a single macro-pulse and multiple macro-pulses at either 40 or 1500 Gy/s, except for minor exceptions. For EBT-XD films, 6.0% of relative difference in the netOD was found at 40 Gy/s for the lowest dose point (2.9 Gy) using the red channel, while 14.2 and 24.9% of relative difference were observed at 1500 Gy/s for that same dose, using red and green channels, respectively. For OC-1 films, 3.8% of relative difference was found at 1500 Gy/s, for 14.7 Gy, using the red channel.

4. Discussion

In this study, we evaluated the dose rate dependency of EBT3, EBT-XD and OC-1 films, for the reference dosimetry of 68 MeV proton beams in UHDR conditions, considering various mean dose rates and beam structures.

We found that above 10 Gy, EBT3 and EBT-XD films showed significant differences of response between conventional (0.25 Gy/s) and UHDR (7500 Gy/s) irradiations, to the contrary of OC-1 films that did not present overall difference of response for doses except below 3 Gy. The response of EBT3 and EBT-XD films was purposely evaluated outside of the dynamic dose ranges indicated by GAFchromic™, with upper limits of 20 and 60 Gy and best performance limits of 10 and 40 Gy, respectively. The impact of the main factors evaluated in this study was found similar between red and green channels for EBT3 and EBT-XD films. The netOD values were consistently higher for UHDR series of irradiations than for conventional ones. This overestimation up to 11% can be far from negligible: once the netOD is converted to dose, using a calibration curve acquired at conventional dose rate, the overestimation of the dose itself could easily exceed 20% in some cases, especially in the dose ranges where the optical density reaches a saturation. For example, the netOD conversion into doses, using the red channel of an EBT-XD film acquired at conventional dose rate for a proton beam irradiation at a mean dose rate of 7500 Gy/s, would lead to a dose overestimation of 8% at 20 Gy and 12% at 60 Gy. The same conversion, using the green channel of an EBT-XD, in the same irradiation conditions, would lead to a dose overestimation of 10.6% at 20 Gy and 15% at 60 Gy, due to a lower saturation in the higher dose regime. When exceeding the dynamic dose range of EBT-XD films, the overestimation of the doses could reach 22.5% and 28.5% at 130 Gy, using the red and green channels, respectively.

No study indicated any variation in the response of EBT3 nor EBT-XD films for electron beams, even at ultra-high mean dose rates, up to 30 Gy [21–23]. For protons, Buonanno et al. irradiated unlaminated EBT3 films at dose rates up to 1000 Gy/s and for doses up to 20 Gy, using a 4.5 MeV proton beam [28]. No influence of the mean dose rate was reported, which is consistent with our findings between 40 and 1500 Gy/s, up to 10 Gy. However, in the present study, we observed an increase of the netOD with the mean dose rate at higher doses for EBT3 films, and more especially between 1500 and 7500 Gy/s. To our knowledge, EBT-XD films have not yet been used for the dosimetry of proton beams in UHDR conditions. Nonetheless, our results showed that even in their dynamic dose range, the use of EBT-XD films in UHDR conditions requires a dedicated calibration curve. Otherwise, the netOD conversion

could also lead to non-negligible overestimations of the dose. Overall, these evaluations of the film response at various mean dose rates suggest that both EBT3 and EBT-XD films should be used with caution for the dosimetry of UHDR proton beams and in the range defined by the manufacturer as "best performances regime".

In this work, we evaluated the response of a new type of radiochromic films, OC-1 films, that present the advantage of a larger dynamic dose range (0.1 – 100 Gy). To our knowledge, no other study of their suitability for the dosimetry of proton beams has yet been conducted. We observed that the mean dose rate had very little impact on OC-1 films in our irradiation conditions, up to 7500 Gy/s, using either red or green channels. In our dose range, the red channel should however preferably be used. Howbeit the vendor indicated a lower limit of the dynamic dose range of 10 cGy, the uncertainty estimated for these films below 10 Gy was quite high, especially using the green channel: 18.8% against 8.2% using the red channel. OC-1 films appear to be suitable for the dosimetry of proton beams in UHDR conditions despite these high uncertainties at low doses and should preferably be used for total delivered dose above 10 Gy. However, their practicality is limited by their unlamination, making them fragile and difficult to handle. Some flaws can easily appear on the films and locally increase the uncertainty on the netOD.

For the comparison of the response of EBT3, EBT-XD and OC-1 films between mean dose rates of 0.25 and 7500 Gy/s, the beam structure was also necessarily varied between single vs. multiple macro-pulses (**Table 1**). In order to study the variation of the structure (intra-pulse dose rate and number of macro-pulses) independently from the mean dose rate, we used the two intermediate mean dose rates: 40 and 1500 Gy/s. When comparing single vs. multiple macro-pulses for a given mean dose rate (40 or 1500 Gy/s), no impact was found associated with the beam structure for the three types of films.

Overall, we also observed differences in the response of the films between EBT (EBT3/EBT-XD) and OC-1 films. The explanation could come from their differences in atomic composition that may influence the localized reaction to the proton beam at ultra-high dose rates. Another difference between these EBT and OC-1 films is the structure of these films: the EBT3 and EBT-XD films that

we used for this study were laminated, with matte polyester layers on both sides of the active layer, while OC-1 films were unlaminated. However, the way those films were systematically stacked during irradiations (EBT3, EBT-XD and OC-1 in the beam axis) limits the impact of unlamination.

Some limitations should be considered in our study. First, the maximum intra-pulse dose rate that we were able to reach with our proton beamline was 7500 Gy/s. If "FLASH" therapy typically involves dose rates > 40 Gy/s and that 7500 Gy/s is certainly considered as an ultra-high dose rate, it is still low compared to what can be reached using laser-accelerated electrons, with intra-pulse dose rates up to $10^9 – 10^{12}$ Gy/s [17]. We plan to explore this issue in more depth once technical limitations are overcome and that higher dose rates than 7500 Gy/s can be generated with our proton beamline. Additional intermediate mean dose rates should also be considered. A second limitation is that we could not precisely reach a targeted dose value with our current setup, and had to fit our data for the comparison. This can introduce a potential source of bias, however very low: the good quality of our fits was verified and no impact on our findings could be detected. Moreover, all our graphical representations (**Figures 3-5**) involve original unfitted data. Finally, a last limitation of this study is that our observations are valid for 68 MeV protons. Further efforts will be made to expand our results to more beam energies or to other particles such as alpha particles.

5. Conclusions

In this study, we investigated the usability of EBT3, EBT-XD and OC-1 radiochromic films, for the reference dosimetry of 68 MeV proton beams in UHDR conditions. We evaluated the dose rate dependency of these films considering various mean dose rates (0.25, 40, 1500 and 7500 Gy/s) on a large dose range (2–130 Gy) and various macro-pulses structures. Our results showed that even in their dynamic dose range, the use of both EBT3 and EBT-XD films in UHDR conditions – above 10 Gy and with a conventional dose rate calibration – could lead to non-negligible overestimations of the netOD and hence the absolute dose, especially with increasing mean dose rates. OC-1 films did not show any impact of the mean dose rate up to 7500 Gy/s, except possibly at very low doses associated to higher uncertainties, for 3 Gy and below.

In conclusion, for typical dose values used in most published studies on the FLASH effect, the response of EBT3 and EBT-XD radiochromic films did not show significant discrepancies between conventional and UHDR irradiations. However, above 10 Gy, these films should be used with caution for the dosimetry of UHDR proton beams. For a proton beam of 68 MeV, their optimal dose range should be limited to 10 Gy, and only for mean dose rates inferior to 1500 Gy/s in the case of EBT3 films. The dose rate dependency of OC-1 films should still be evaluated at UHDR > 7500 Gy/s and a broader investigation of their usability for the dosimetry of UHDR proton beams should be conducted at other beam energies. In our future experiments in UHDR conditions, we will select the radiochromic film in use depending on the studied dose, in order to insure the quality of our results and limit overestimation: EBT3 or EBT-XD films up to 10 Gy, and OC-1 between 10 and 100 Gy.

References

1. Berry RJ, Hall EJ, Forster DW, Storr TH, Goodman MJ. Survival of mammalian cells exposed to x rays at ultra-high dose-rates. *Br J Radiol*. 1969;42(494):102-107. doi:10.1259/0007-1285-42-494-102

2. Favaudon V, Caplier L, Monceau V, et al. Ultrahigh dose-rate FLASH irradiation increases the differential response between normal and tumor tissue in mice. *Sci Transl Med*. 2014;6(245):245ra93. doi:10.1126/scitranslmed.3008973

3. Durante M, Bräuer-Krisch E, Hill M. Faster and safer? FLASH ultra-high dose rate in radiotherapy. *Br J Radiol*. 2018;91(1082):20170628. doi:10.1259/bjr.20170628

4. Vozenin MC, De Fornel P, Petersson K, et al. The Advantage of FLASH Radiotherapy Confirmed in Mini-pig and Cat-cancer Patients. *Clin Cancer Res Off J Am Assoc Cancer Res*. 2019;25(1):35-42. doi:10.1158/1078-0432.CCR-17-3375

5. Vozenin MC, Hendry JH, Limoli CL. Biological Benefits of Ultra-high Dose Rate FLASH Radiotherapy: Sleeping Beauty Awoken. *Clin Oncol R Coll Radiol G B*. 2019;31(7):407-415. doi:10.1016/j.clon.2019.04.001

6. Bourhis J, Sozzi WJ, Jorge PG, et al. Treatment of a first patient with FLASH-radiotherapy. *Radiother Oncol J Eur Soc Ther Radiol Oncol*. 2019;139:18-22. doi:10.1016/j.radonc.2019.06.019

7. Town CD. Effect of High Dose Rates on Survival of Mammalian Cells. *Nature*. 1967;215(5103):847-848. doi:10.1038/215847a0

8. Auer S, Hable V, Greubel C, et al. Survival of tumor cells after proton irradiation with ultra-high dose rates. *Radiat Oncol Lond Engl*. 2011;6:139. doi:10.1186/1748-717X-6-139

9. Levy K, Natarajan S, Wang J, et al. Abdominal FLASH irradiation reduces radiation-induced gastrointestinal toxicity for the treatment of ovarian cancer in mice. *Sci Rep*. 2020;10(1):21600. doi:10.1038/s41598-020-78017-7

10. Fouillade C, Curras-Alonso S, Giuranno L, et al. FLASH Irradiation Spares Lung Progenitor Cells and Limits the Incidence of Radio-induced Senescence. *Clin Cancer Res Off J Am Assoc Cancer Res*. 2020;26(6):1497-1506. doi:10.1158/1078-0432.CCR-19-1440

11. Montay-Gruel P, Petersson K, Jaccard M, et al. Irradiation in a flash: Unique sparing of memory in mice after whole brain irradiation with dose rates above 100Gy/s. *Radiother Oncol J Eur Soc Ther Radiol Oncol*. 2017;124(3):365-369. doi:10.1016/j.radonc.2017.05.003

12. Montay-Gruel P, Acharya MM, Petersson K, et al. Long-term neurocognitive benefits of FLASH radiotherapy driven by reduced reactive oxygen species. *Proc Natl Acad Sci*. 2019;116(22):10943-10951.

13. Diffenderfer ES, Verginadis II, Kim MM, et al. Design, Implementation, and in Vivo Validation of a Novel Proton FLASH Radiation Therapy System. *Int J Radiat Oncol Biol Phys*. 2020;106(2):440-448. doi:10.1016/j.ijrobp.2019.10.049

14. International Atomic Energy Agency. *Absorbed Dose Determination in External Beam Radiotherapy, Technical Reports Series No. 398*. IAEA; 2001.

15. McManus M, Romano F, Lee ND, et al. The challenge of ionisation chamber dosimetry in ultra-short pulsed high dose-rate Very High Energy Electron beams. *Sci Rep*. 2020;10(1):9089. doi:10.1038/s41598-020-65819-y

16. Petersson K, Jaccard M, Germond JF, et al. High dose-per-pulse electron beam dosimetry — A model to correct for the ion recombination in the Advanced Markus ionization chamber. *Med Phys*. 2017;44(3):1157-1167. doi:https://doi.org/10.1002/mp.12111

17. Schüller A, Heinrich S, Fouillade C, et al. The European Joint Research Project UHDpulse - Metrology for advanced radiotherapy using particle beams with ultra-high pulse dose rates. *Phys Medica PM Int J Devoted Appl Phys Med Biol Off J Ital Assoc Biomed Phys AIFB*. 2020;80:134-150. doi:10.1016/j.ejmp.2020.09.020

18. Sorriaux J, Kacperek A, Rossomme S, et al. Evaluation of Gafchromic® EBT3 films characteristics in therapy photon, electron and proton beams. *Phys Med*. 2013;29(6):599-606. doi:10.1016/j.ejmp.2012.10.001

19. Castriconi R, Ciocca M, Mirandola A, et al. Dose-response of EBT3 radiochromic films to proton and carbon ion clinical beams. *Phys Med Biol*. 2017;62(2):377-393. doi:10.1088/1361-6560/aa5078

20. Karsch L, Beyreuther E, Burris-Mog T, et al. Dose rate dependence for different dosimeters and detectors: TLD, OSL, EBT films, and diamond detectors. *Med Phys*. 2012;39(5):2447-2455. doi:10.1118/1.3700400

21. Jaccard M, Petersson K, Buchillier T, et al. High dose-per-pulse electron beam dosimetry: Usability and dose-rate independence of EBT3 Gafchromic films. *Med Phys*. 2017;44(2):725-735. doi:10.1002/mp.12066

22. Jorge PG, Jaccard M, Petersson K, et al. Dosimetric and preparation procedures for irradiating biological models with pulsed electron beam at ultra-high dose-rate. *Radiother Oncol*. 2019;139:34-39. doi:10.1016/j.radonc.2019.05.004

23. Favaudon V, Lentz JM, Heinrich S, et al. Time-resolved dosimetry of pulsed electron beams in very high dose-rate, FLASH irradiation for radiotherapy preclinical studies. *Nucl Instrum Methods Phys Res Sect Accel Spectrometers Detect Assoc Equip*. 2019;944:162537. doi:10.1016/j.nima.2019.162537

24. Patriarca A, Fouillade C, Auger M, et al. Experimental Set-up for FLASH Proton Irradiation of Small Animals Using a Clinical System. *Int J Radiat Oncol Biol Phys*. 2018;102(3):619-626. doi:10.1016/j.ijrobp.2018.06.403

25. Beyreuther E, Brand M, Hans S, et al. Feasibility of proton FLASH effect tested by zebrafish embryo irradiation. *Radiother Oncol J Eur Soc Ther Radiol Oncol*. 2019;139:46-50. doi:10.1016/j.radonc.2019.06.024

26. Cunningham S, McCauley S, Vairamani K, et al. FLASH Proton Pencil Beam Scanning Irradiation Minimizes Radiation-Induced Leg Contracture and Skin Toxicity in Mice. *Cancers*. 2021;13(5):1012. doi:10.3390/cancers13051012

27. Zhang Q, Cascio E, Li C, et al. FLASH Investigations Using Protons: Design of Delivery System, Preclinical Setup and Confirmation of FLASH Effect with Protons in Animal Systems. *Radiat Res*. 2020;194(6):656-664. doi:10.1667/RADE-20-00068.1

28. Buonanno M, Grilj V, Brenner DJ. Biological effects in normal cells exposed to FLASH dose rate protons. *Radiother Oncol J Eur Soc Ther Radiol Oncol*. 2019;139:51-55. doi:10.1016/j.radonc.2019.02.009

29. Esplen N, Mendonca MS, Bazalova-Carter M. Physics and biology of ultrahigh dose-rate (FLASH) radiotherapy: a topical review. *Phys Med Biol*. 2020;65(23):23TR03. doi:10.1088/1361-6560/abaa28

30. Koumeir C, De Nadal V, Cherubini R, et al. THE RADIOBIOLOGICAL PLATFORM AT ARRONAX. *Radiat Prot Dosimetry*. 2019;183(1-2):270-273. doi:10.1093/rpd/ncy301

31. Poirier F, Blain G, Bulteau-Harel F, et al. The Pulsing Chopper-Based System of the Arronax C70XP Cyclotron. *Proc 10th Int Part Accel Conf*. 2019;IPAC2019. doi:10.18429/JACOW-IPAC2019-TUPTS008

32. Poirier F, Blain G, Bulteau-Harel F, et al. The Injection and Chopper-Based System at Arronax C70XP Cyclotron. *Proc 22nd Int Conf Cyclotr Their Appl*. 2020;Cyclotrons2019. doi:10.18429/JACOW-CYCLOTRONS2019-TUP006

33. Bongrand A, Koumeir C, Villoing D, et al. A Monte Carlo Determination of Dose and Range Uncertainties for Preclinical Studies with a Proton Beam. *Cancers*. 2021;13(8):1889. doi:10.3390/cancers13081889

34. Lill JO. Charge integration in external-beam PIXE. *Nucl Instrum Methods Phys Res Sect B Beam Interact Mater At*. 1999;150(1):114-117. doi:10.1016/S0168-583X(98)01074-X

35. Ashland. Gafchromic EBT3 specifications. Published 2020. Accessed June 21, 2021. http://www.gafchromic.com/documents/EBT3_Specifications.pdf

36. Ashland. Gafchromic EBT-XD specifications. Published 2020. Accessed June 21, 2021. http://www.gafchromic.com/documents/EBTXD_Specifications.pdf

37. Micke A, Yu X. OrthoChromic Film Dosimetry Protocol. Published online 2020. http://www.orthochromic.com/OC/Documents/OCI_Protocol_2020_Full.pdf

Acknowledgments

This work was partially funded by Equipex ARRONAX-Plus (ANR-11-EQPX-0004), Labex IRON (ANR-11-LABX-18-01), ISITE NExT (ANR-16-IDEX-0007), and with financial support from Inserm Cancer.

Conflicts of interest

The authors declare no conflict of interest.

Figure captions

Figure 1. Proton beam experimental setup. K = Kapton (beam exit window); TF = Tungsten foil; C1 = 1st collimator Ø 15 mm; PM = Photomultiplier tube; C2 = 2nd collimator Ø 10 mm; IC = ionization chamber; FC = Faraday cup Ø 30 mm.

Figure 2. Beam structure variations for (a) experiment #1 (variation of intensity, number of macro-pulses and frequency), (b) experiment #2 (single pulse, variation of intensity and macro-pulse width) and (c) experiment #3 (variation of macro-pulse frequency).

Figure 3. Evaluation of the differences in film response between conventional (0.25 Gy/s) and ultra-high dose rates (7500 Gy/s), for EBT3, EBT-XD and OC-1 films, using the red channel of these films.

Figure 4. Influence of the mean dose rate on the response of EBT3 (A), EBT-XD (B) and OC-1 (C) films, at mean dose rates of 40, 1500 and 7500 Gy/s, using both red and green channels.

Figure 5. Influence of the beam structure on the response of EBT3 (A), EBT-XD (B) and OC-1 (C) films, at a mean dose rate of 40 Gy/s, for a single pulse (intra-pulse dose rate of 40 Gy/s) and multiple pulses (intra-pulse dose rates of 7500 Gy/s), using both red and green channels.

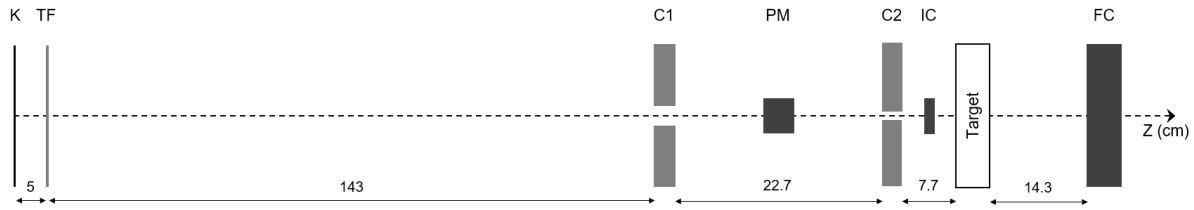

Figure 1. Proton beam experimental setup. K = Kapton (beam exit window); TF = Tungsten foil; C1 = 1st collimator Ø 15 mm; PM = Photomultiplier tube; C2 = 2nd collimator Ø 10 mm; IC = ionization chamber; FC = Faraday cup Ø 30 mm.

Table 1. Beam structures of experiments #1, #2 and #3.

	Mean dose rate (Gy/s)	**Intra-pulse dose rate (Gy/s)**	**Number of macro-pulses**	**Macro-pulse width (ms)**	**Macro-pulse repetition frequency (Hz)**
Experiment	7500	7500	1	0.27 – 16.67	-
#1	0.25	6.3	800 – 50000	0.4	100
Experiment	40	40	1	75 – 3000	-
#2	1500	1500	1	2 – 80	-
	7500	7500	1	0.27 – 16.67	-
Experiment	40	7500	4 – 160	0.1	53.3
#3	1500	7500	4 – 160	0.1	2000

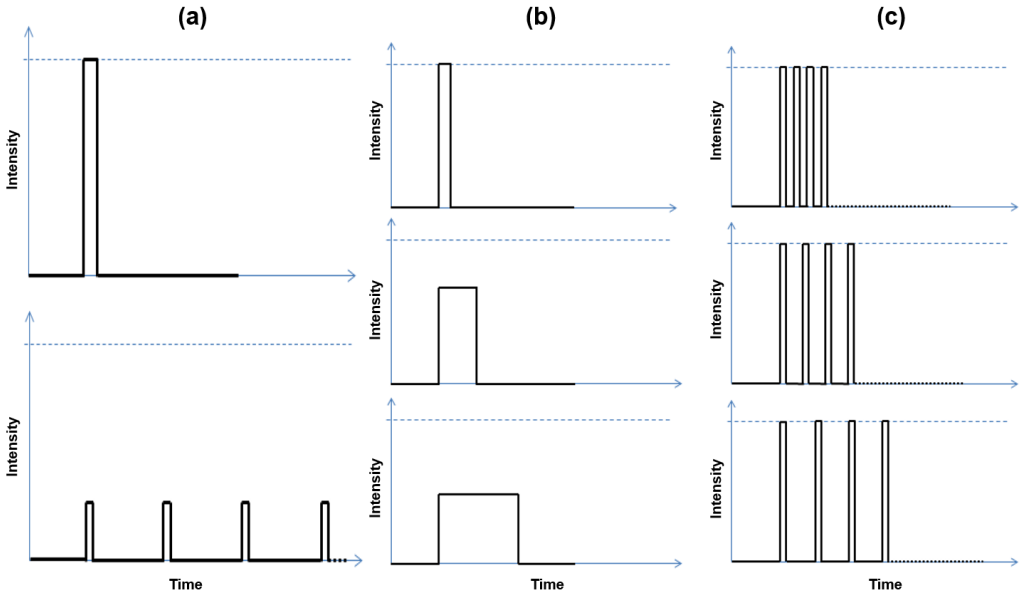

Figure 2. Beam structure variations for (a) experiment #1 (variation of intensity, number of macro-pulses and frequency), (b) experiment #2 (single pulse, variation of intensity and macro-pulse width) and (c) experiment #3 (variation of macro-pulse frequency).

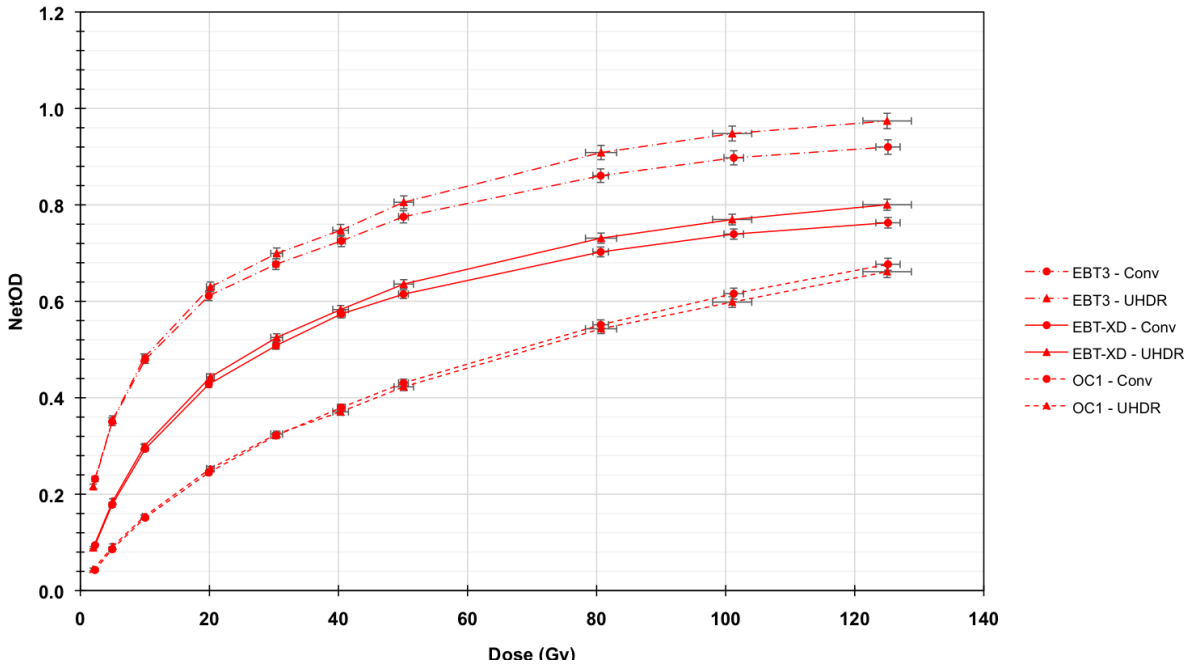

Figure 3. Evaluation of the differences in film response between conventional (0.25 Gy/s) and ultra-high dose rates (7500 Gy/s), for EBT3, EBT-XD and OC-1 films, using the red channel of these films.

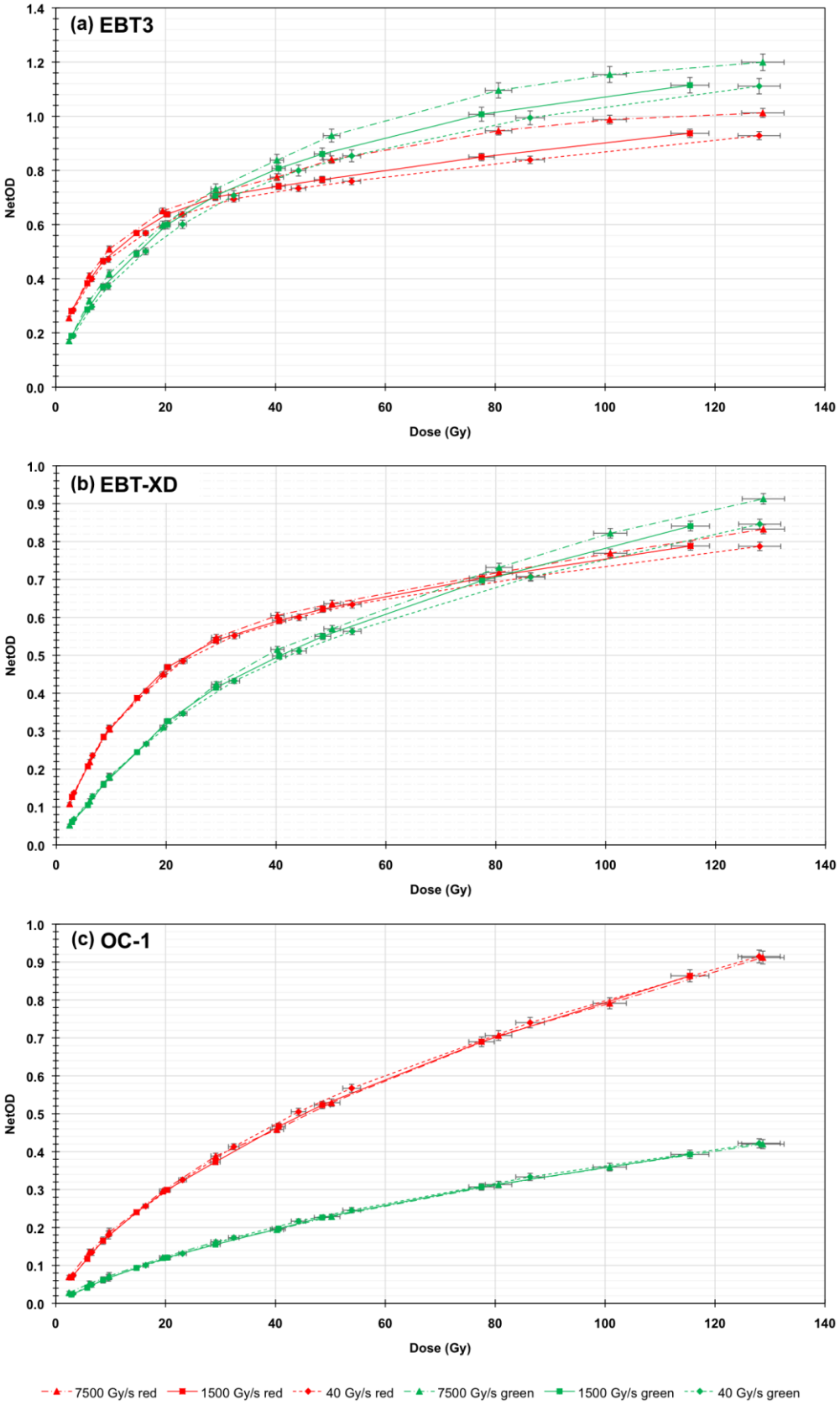

Figure 4. Influence of the mean dose rate on the response of EBT3 (A), EBT-XD (B) and OC-1 (C) films, at mean dose rates of 40, 1500 and 7500 Gy/s, using both red and green channels.

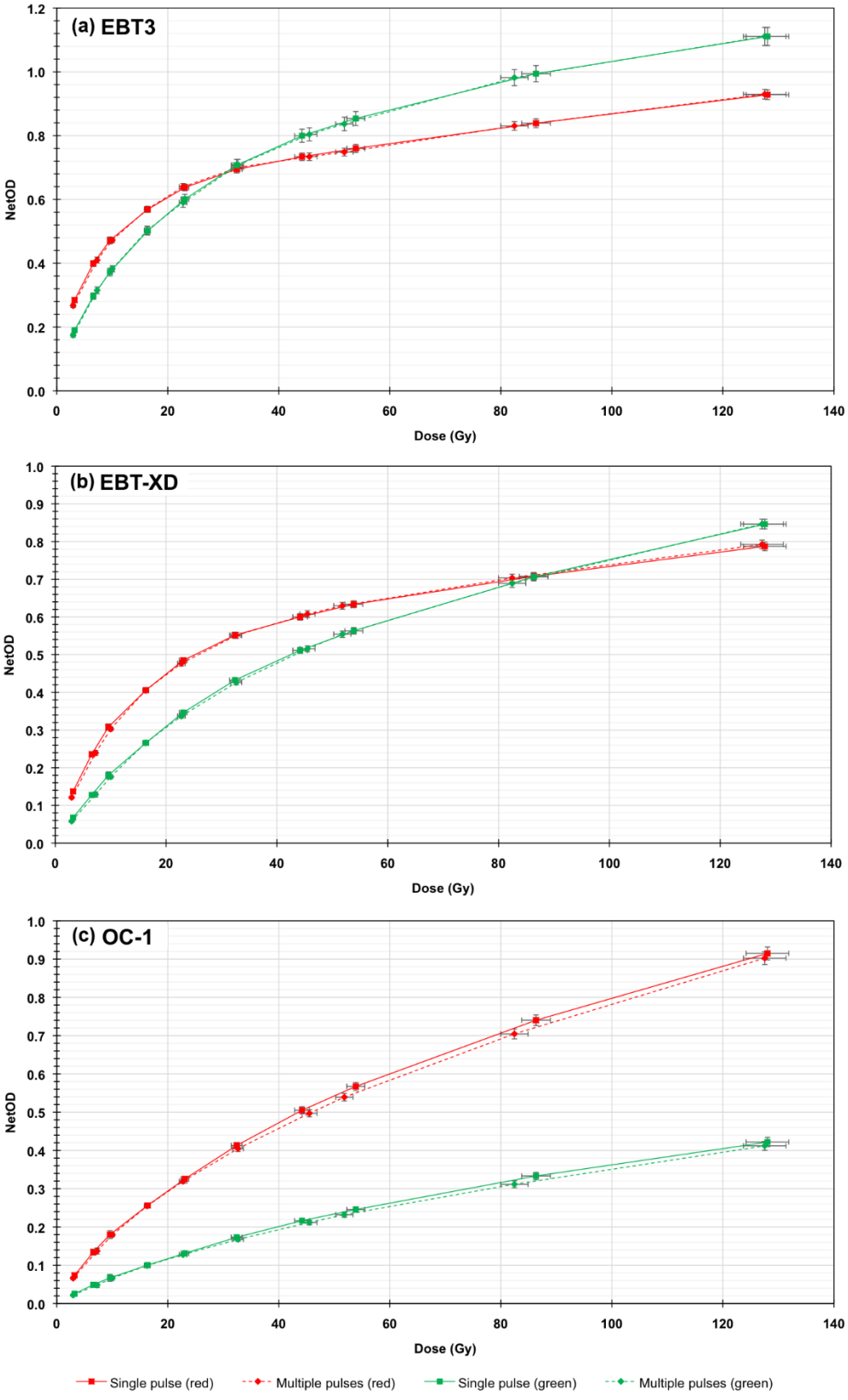

Figure 5. Influence of the beam structure on the response of EBT3 (A), EBT-XD (B) and OC-1 (C) films, at a mean dose rate of 40 Gy/s, for a single pulse (intra-pulse dose rate of 40 Gy/s) and multiple pulses (intra-pulse dose rates of 7500 Gy/s), using both red and green channels.